BNL-105243-2014-TECH

Booster Technical Note No. 199;BNL-105243-2014-IR

BOOSTER HEAVY ION ACCELERATION CYCLES WITH CHANGE OF HARMONIC

D. P. Deng

September 1991

Collider Accelerator Department

Brookhaven National Laboratory

U.S. Department of Energy

USDOE Office of Science (SC)

DISCLAIMER

BOOSTER HEAVY ION ACCELERATION CYCLES

WITH CHANGE OF HARMONIC

BOOSTER TECHNICAL NOTE
NO. 199

D. P. DENG and J. M. BRENNAN

SEPTEMBER 12, 1991

ALTERNATING GRADIENT SYNCHROTRON DEPARTMENT
BROOKHAVEN NATIONAL LABORATORY
UPTON, NEW YORK 11973

Booster Heavy Ion Acceleration Cycles with Change of Harmonic Numbers

D.-P. Deng and J.M. Brennan
Brookhaven National Laboratory
Upton, Long Island, NY 11973

August 29, 1991

1 Introduction

To accelerate heavy ions in the Booster with the third harmonic system, the original Booster Design Manual calls for constructions of two Band I , one Band II and two Band III cavities. Band I, II and III cavities cover frequency ranges from 178kHz to 675kHz, from 600kHz to 2.5MHz and from 2.4MHz to 4.2MHz respectively. Now it is decided to build two Band II cavities and utilize them along with two Band III cavities to accelerate heavy ions. The modified acceleration scenario goes as follows. Step 1 is to use Band II with a higher harmonic number to capture and accelerate heavy ions; step 2 is to debunch the beam when the RF frenquency reaches $2.4MHz$; the final step is to use Band II to recapture and accelerate heavy ions with harmonic number 3, and as the RF frequency reaches $2.4MHz$, Band III starts to take over and accelerate heavy ions to their top energy. Note the third harmonic system spans over Band II and Band III.

This note designs acceleration cycles for silicon ions Si^{+14} and gold ions Au^{+33}. For Au^{+33}, cycles with harmonic number 12 and 9 are presented. For Si^{+14}, a cycle with harmonic number 6 is presented.

2 Capture and Longitudinal Emittance

Since the heavy ion beams from the Tandem Van de Graaff have virtually zero energy spread, the initial bucket area at capture determines the initial longitudinal emittance. If adiabaticity applies, the longitudinal emittance is conserved throughout the cycle. We may take the initial bucket area at capture as the longitudinal emittance in the higher harmonic system. The total emittance, being the sum of the emittances of all bunches, is assumed to be a constant. Before and after the change of harmonic number, the total emittance is equally distributed in the bunches.

Let's take a look at the dependence of the final emittance (in unit eVs) in the third harmonic system on the initial higher harmonic number. The initial longitudinal emittance is taken as the bucket area at injection, which has a dependence on the harmonic number as $h^{-\frac{3}{2}}$. Then the final emittance will be proportional to $h * h^{-\frac{3}{2}} = h^{-\frac{1}{2}}$. So provided everything else is the same, the final emittance in the third harmonic system is inversely proportional to the square root of the initial harmonic number. The higher the initial harmonic number, the smaller the final emittance.

If the capture takes place at constant magnetic field, the initial and the final emittance vary as the sqare root of the initial voltage. The smaller the voltage, the smaller the emittance.

3 Acceleration Cycles

To reduce the loss of particles at capture, it is prefered to use a stationary bucket. However, for the ease of injection process, a moving bucket with small synchronous phase angle is adopted in this note.

The injection time window is assumed to be $30ms$, injection can happen at any moment in this time interval. The time to ramp up and ramp down for the cavity voltages is assumed as 5 times of the synchrotron oscillation period, *i.e.* $\frac{5}{f_\nu}$, where f_ν is evaluated at the maximum of RF voltage; the time period to ramp up and ramp down of the rate of change of the magnetic field is taken as $10ms$; the coasting time is $50ms$ and is a very conservative estimate of the time needed to retune the Band II cavities. The form of ramp up (down) for the voltage and the rate of change of magnetic field is a portion of sine function from valley to peak (from peak to valley). Thus the variation of the voltage and the rate of change of the magnetic field is a continuous and smooth function.

The important parameters presented in this note are RF frequency f_{rf}, $\dot{\mathcal{B}}$, dipole field $\mathcal{B}$, kinetic energy K, bucket area A_{bkt}, synchronous phase angle ϕ_s, voltage V_{rf}, synchrotron oscillation frequency f_ν, bucket length and bunch length.

At injection, the $\dot{\mathcal{B}}$ is set at $0.05T/s$. After the injection period ($30ms$), $\dot{\mathcal{B}}$ ramps up to $2.5T/s$ and then stays at that value. When the RF frenquency approaches $2.4MHz$, $\dot{\mathcal{B}}$ starts to ramp down and reaches zero when the RF frenquency is $2.4MHz$. The initial RF voltage is set at $1.0kV$, then it is ramped up to $15.0kV$ in roughly $2ms$ (five times of the synchrotron oscillation period) and sustains. When $\dot{\mathcal{B}}$ is reduced to zero, the voltage is then ramped down to zero as the debunching process takes place. The RF frequency program is changed to the new harmonic number while the Gauss clock continues to track small variations in the magnetic field. The cavity is retuned to the new RF frequency and the voltage is ramped from zero up to $15.0kV$. When the voltage gains a value of $15.0kV$, $\dot{\mathcal{B}}$ starts to ramp up to $2.5T/s$.

Figures (1)—(12) depict the process for a harmonic number $h = 12$. The final longitudinal emittance is $3.9eVs$ (or $0.020eVs/u$). Figures (13)—(24) depict the process for a harmonic number $h = 9$. The final longitudinal emittance is $4.5eVs$ (or $0.023eVs/u$). Note during the debunching period including the end points, the bucket areas, bucket lengths and bunch lengths are all set to zero.

Figures (25)—(36) depict the process for a harmonic number $h = 6$ for Si^{+14}, the final emittance is $1.37eVs$ (or $0.049eVs/u$). As a side note, harmonic number 4 or 5 can also be used in order to use a wider frequency range in Band II; though the final emittance would be a little larger.

	β	f_{inj} (MHz) $h = 12$	f_{inj} (MHz) $h = 9$	f_{inj} (MHz) $h = 6$	E_{inj} (GeV)	B_{inj} (T)	f_{ej} (MHz)	E_{ej} (GeV)	B_{ej} (T)
Si^{+14}	0.1194			1.0643	0.188	0.05428	4.0	32.86	0.9184
Au^{+33}	0.0478	0.8524	0.6393		0.210	0.0645	3.061	68.95	1.2743

Table 1: Some parameters at injection and ejection.

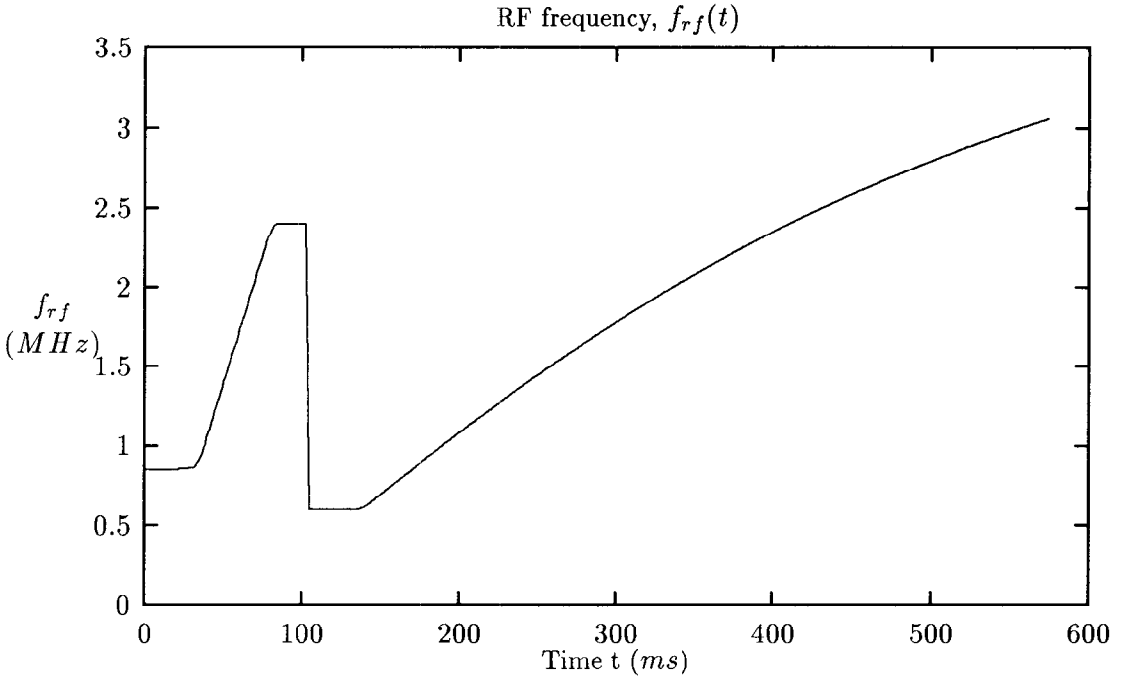

Figure 1: RF frequency *vs.* time

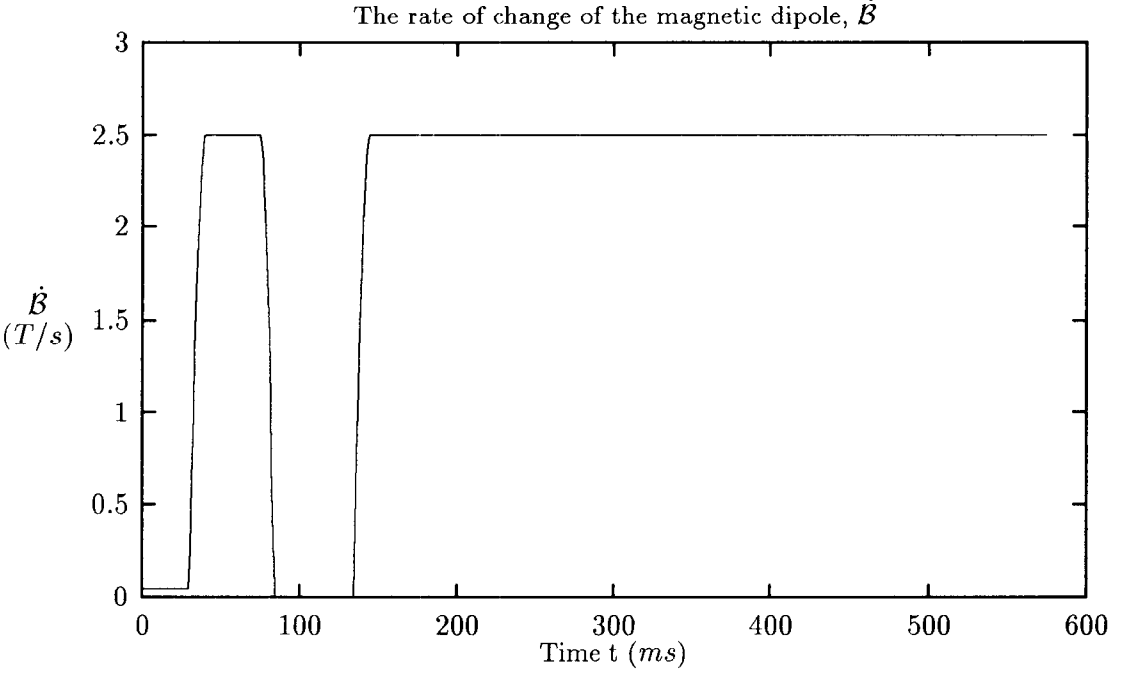

Figure 2: The rate of change of the magnetic dipole field *vs.* time. $Au^{+33}, h = 12$.

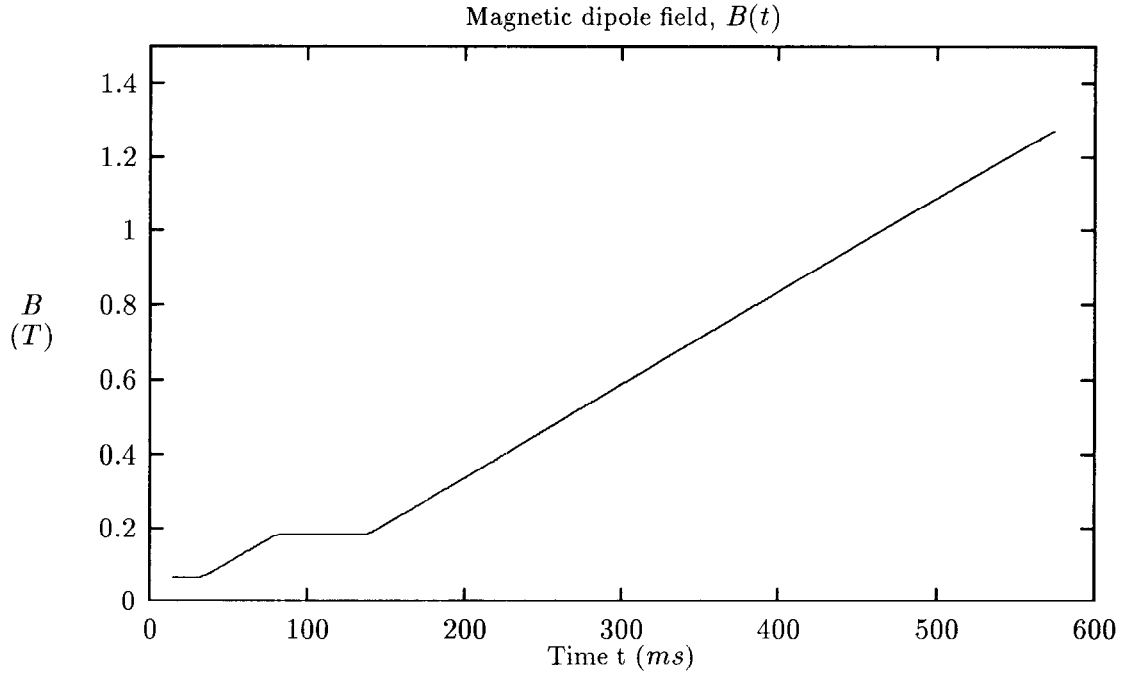

Figure 3: The magnetic dipole field *vs.* time. $Au^{+33}, h = 12$.

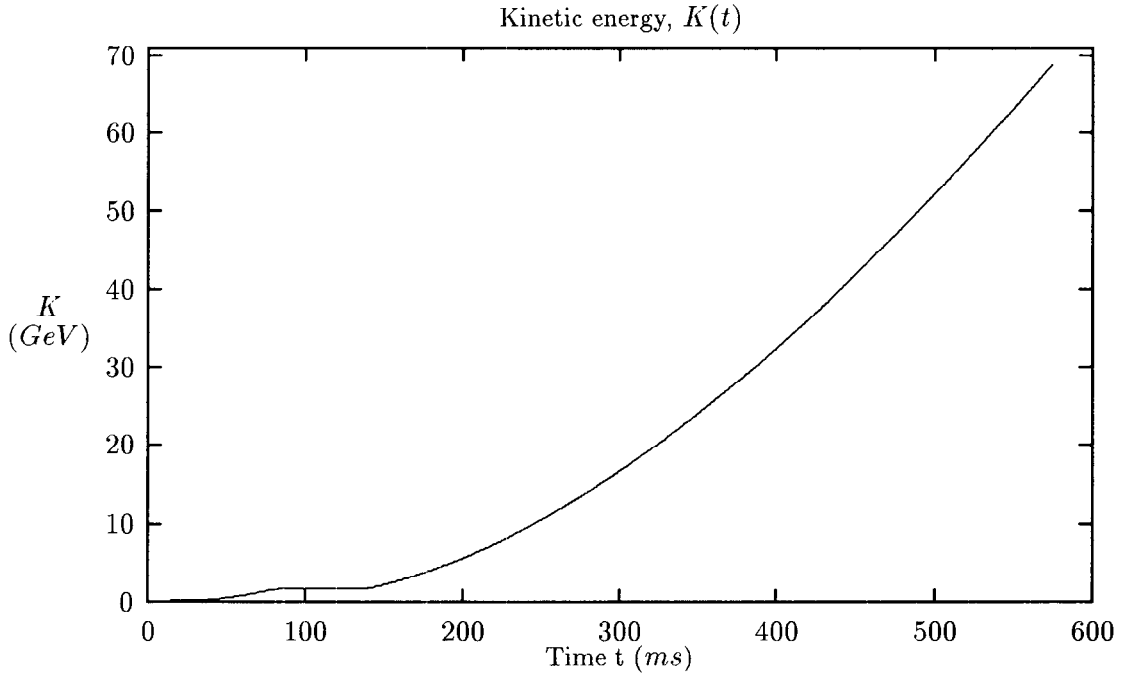

Figure 4: Kinetic energy *vs.* time. $Au^{+33}, h = 12$.

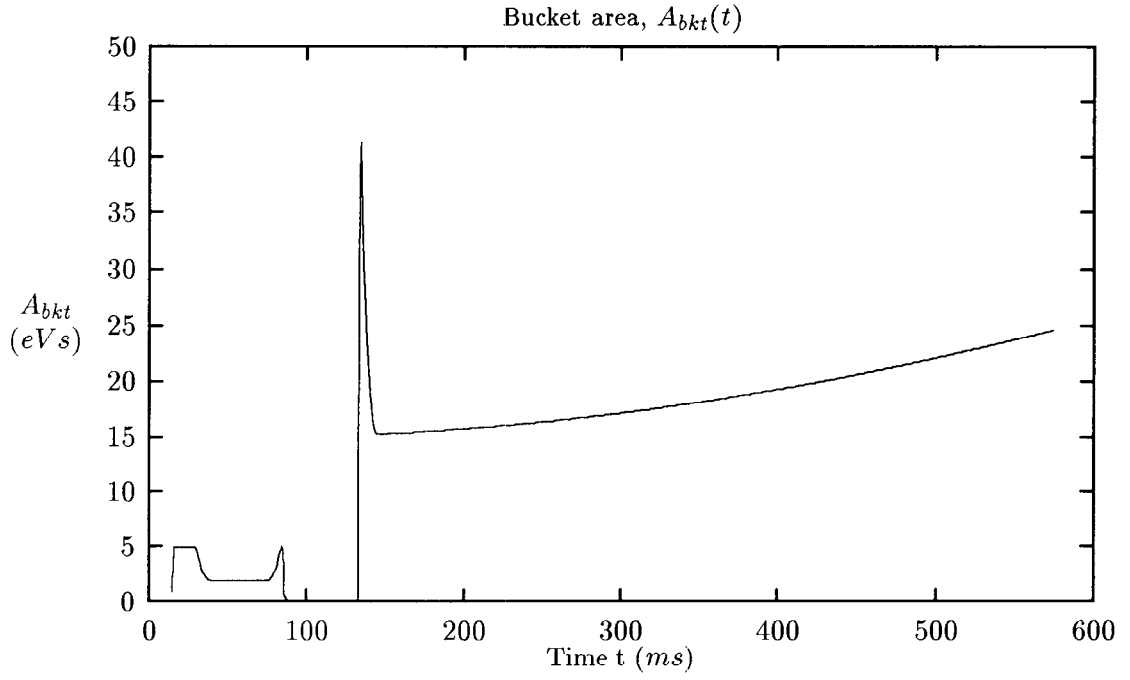

Figure 5: The bucket area *vs.* time. $Au^{+33}, h = 12$.

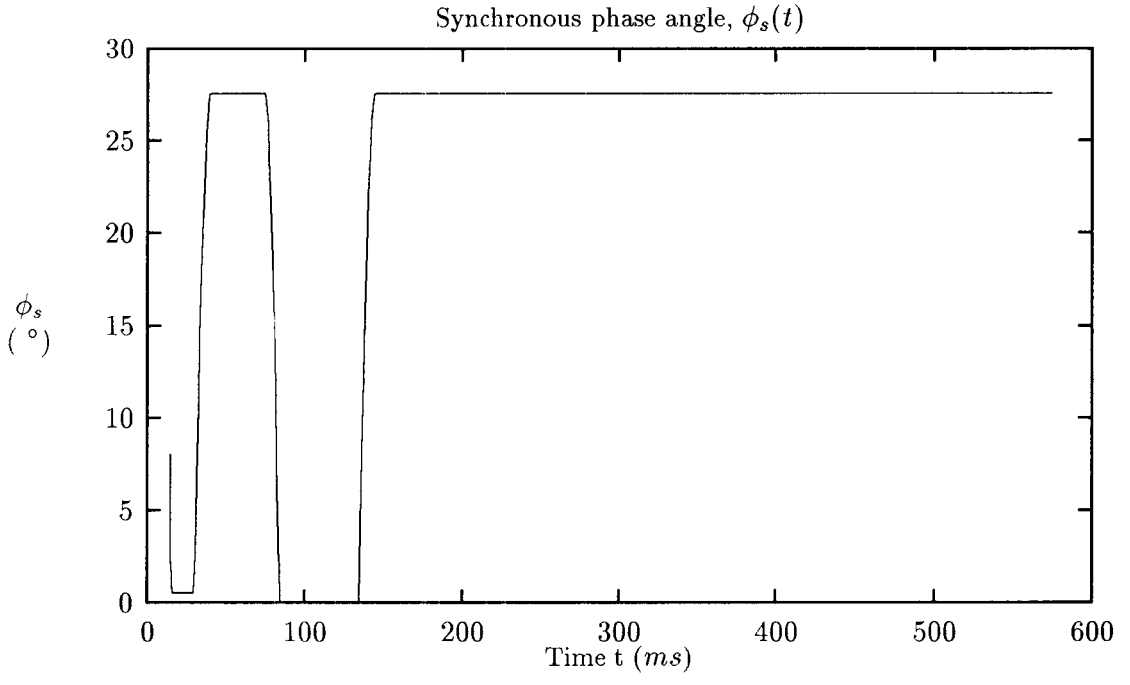

Figure 6: Synchronous phase angle *vs.* time. $Au^{+33}, h = 12$.

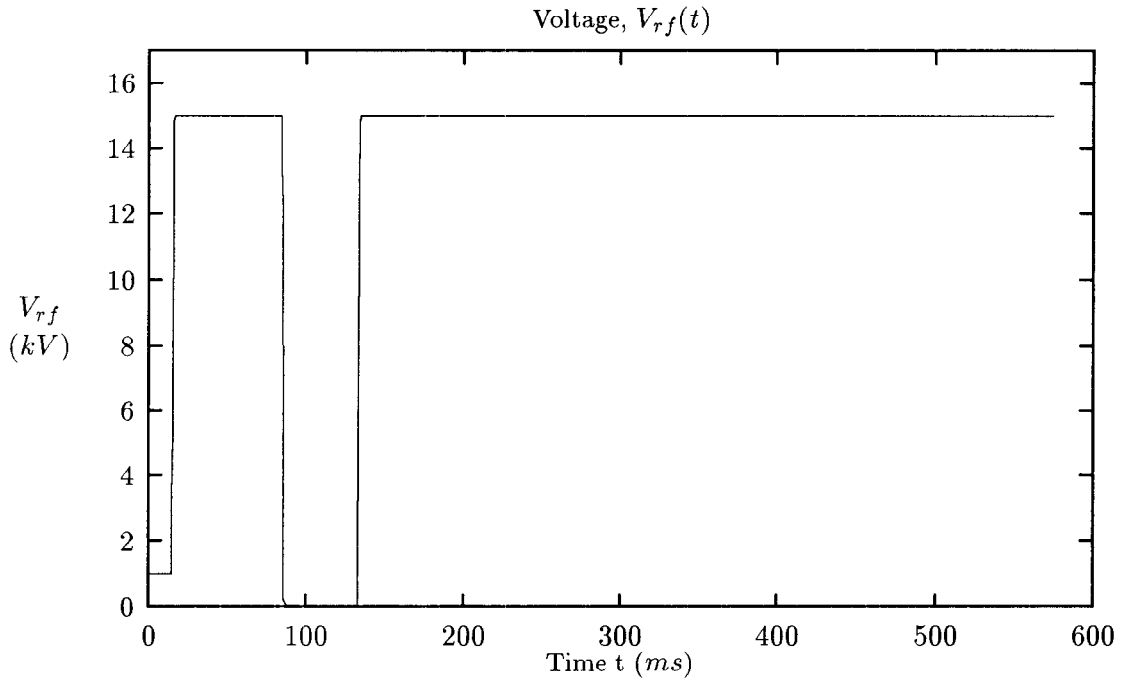

Figure 7: RF voltage *vs.* time. $Au^{+33}, h = 12$.

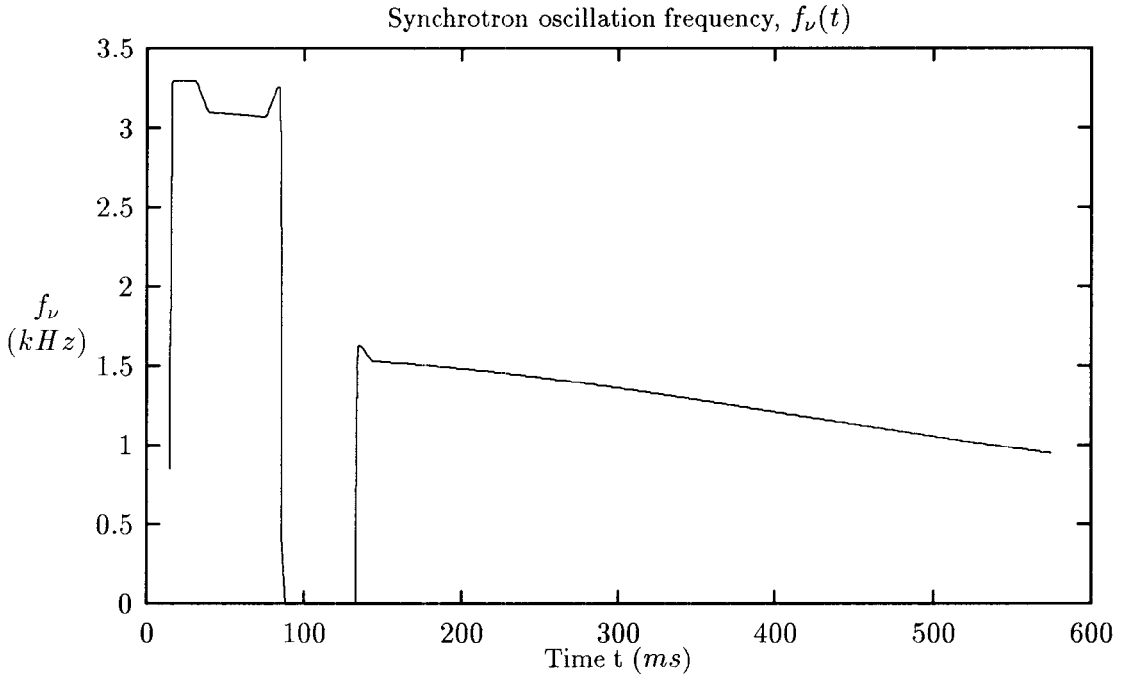

Figure 8: Synchrotron oscillation frequency *vs.* time. $Au^{+33}, h = 12$.

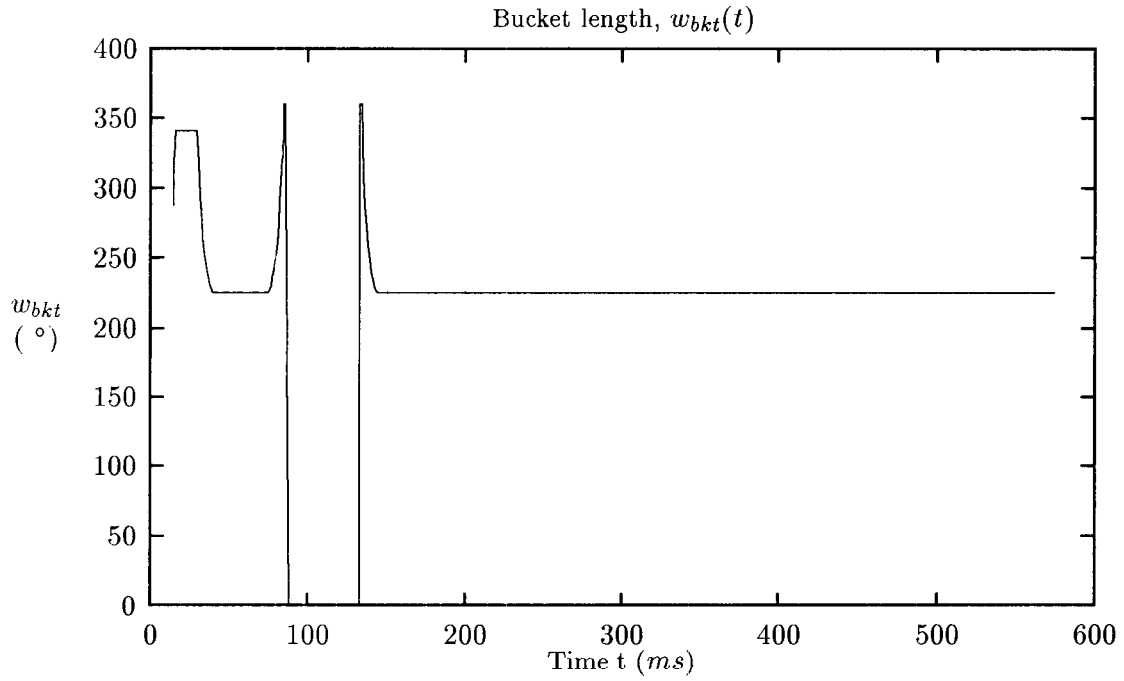

Figure 9: Bucket length (degree) *vs.* time. $Au^{+33}, h = 12$.

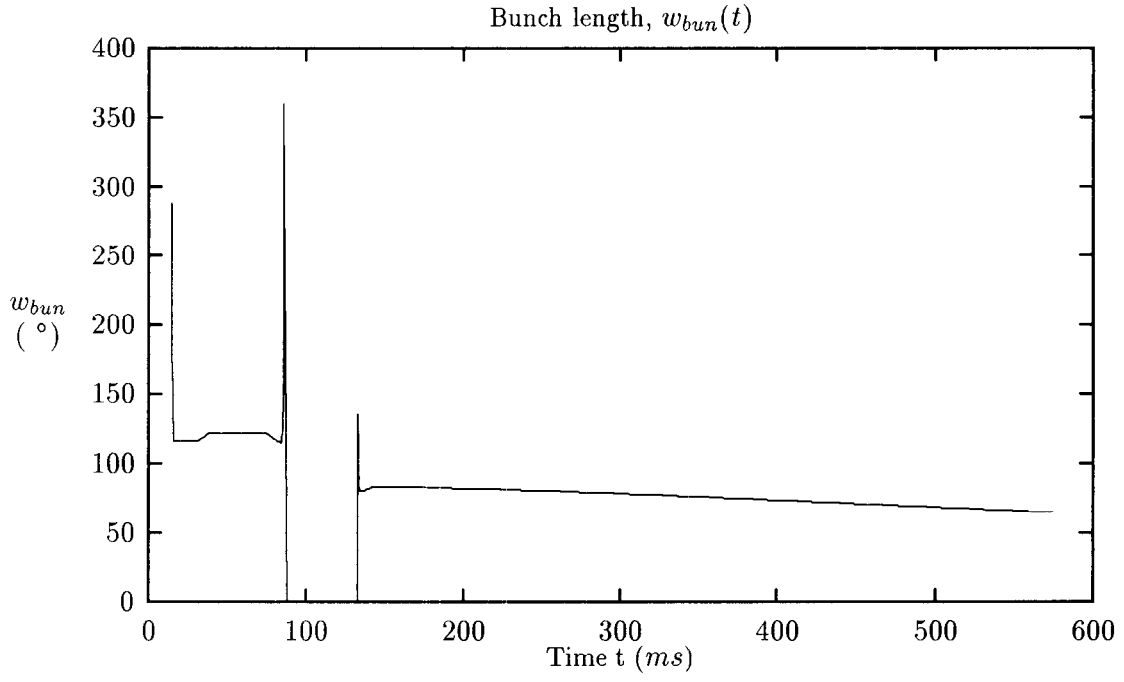

Figure 10: Bunch length (degree) *vs.* time. $Au^{+33}, h = 12$.

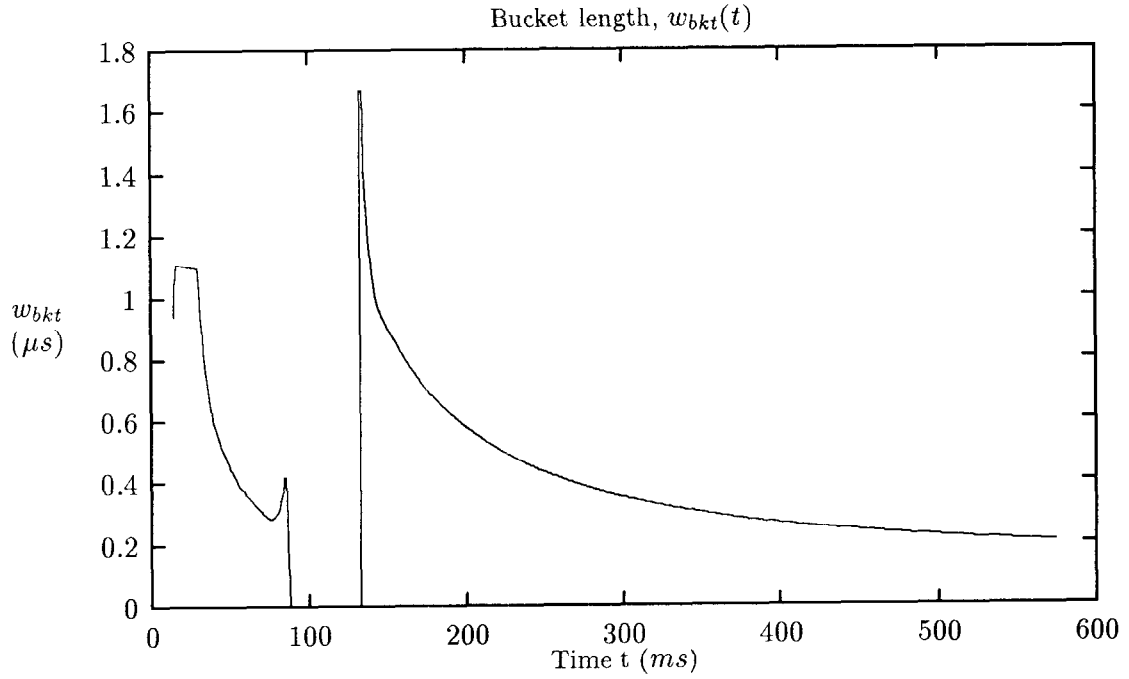

Figure 11: Bucket length (ms) *vs.* time. $Au^{+33}, h = 12$.

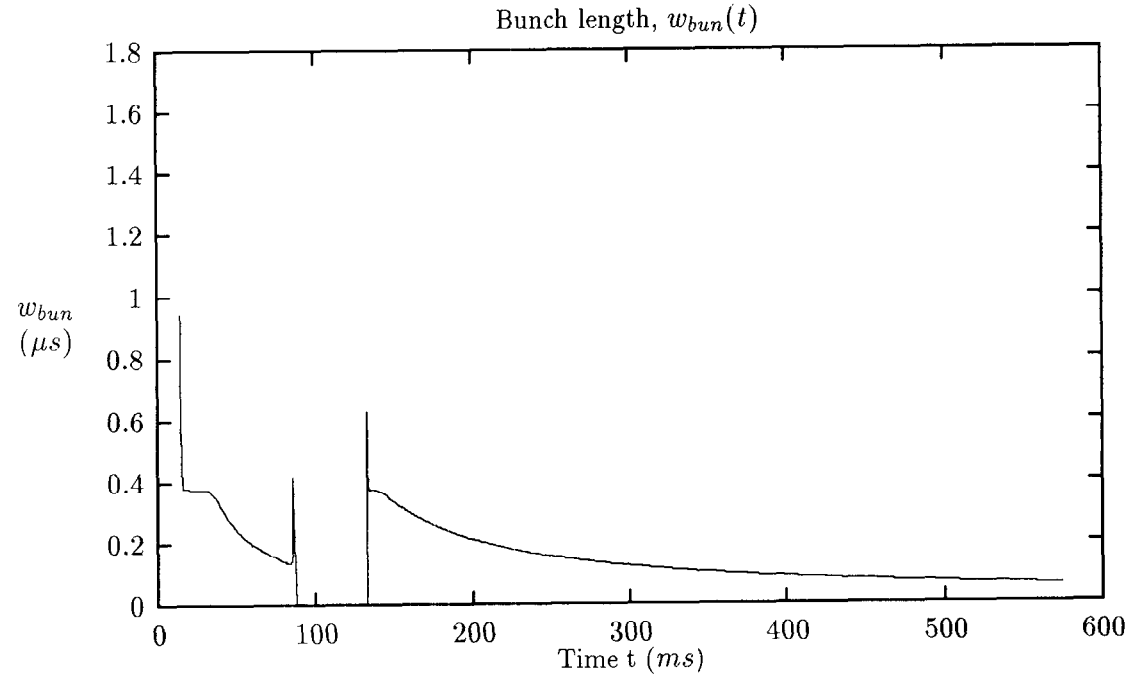

Figure 12: Bunch length (ms) *vs.* time. $Au^{+33}, h = 12$.

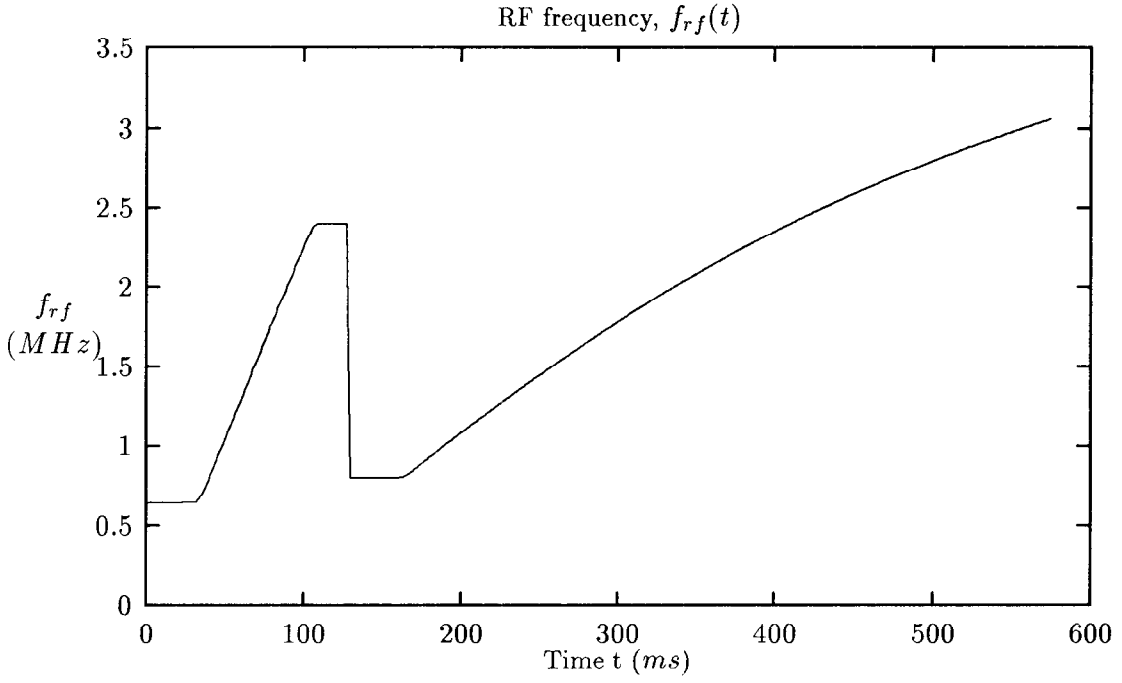

Figure 13: RF frequency *vs.* time. $Au^{+33}, h = 9$.

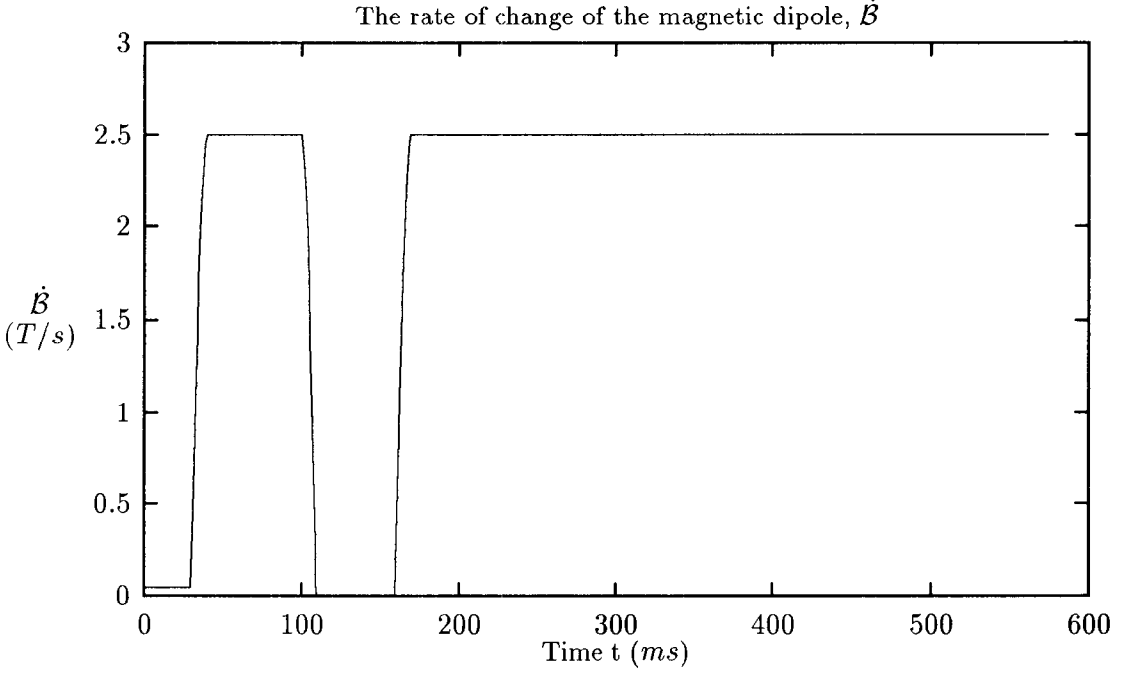

Figure 14: The rate of change of the magnetic dipole field *vs.* time. $Au^{+33}, h = 9$.

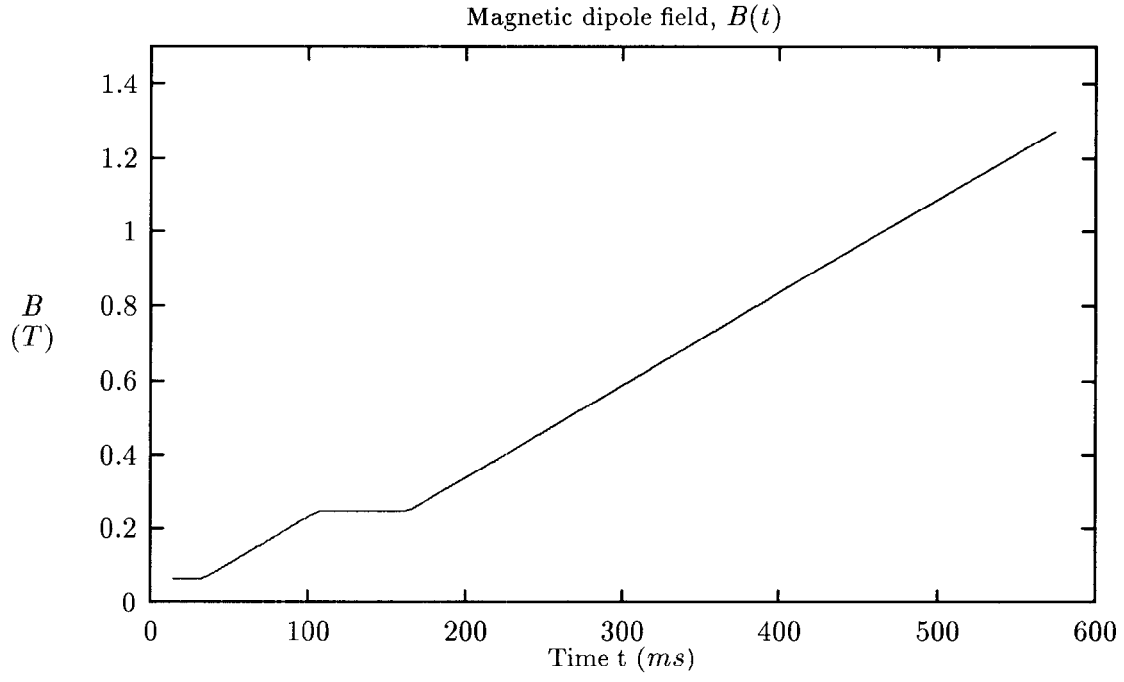

Figure 15: The magnetic dipole field *vs.* time. $Au^{+33}, h = 9$.

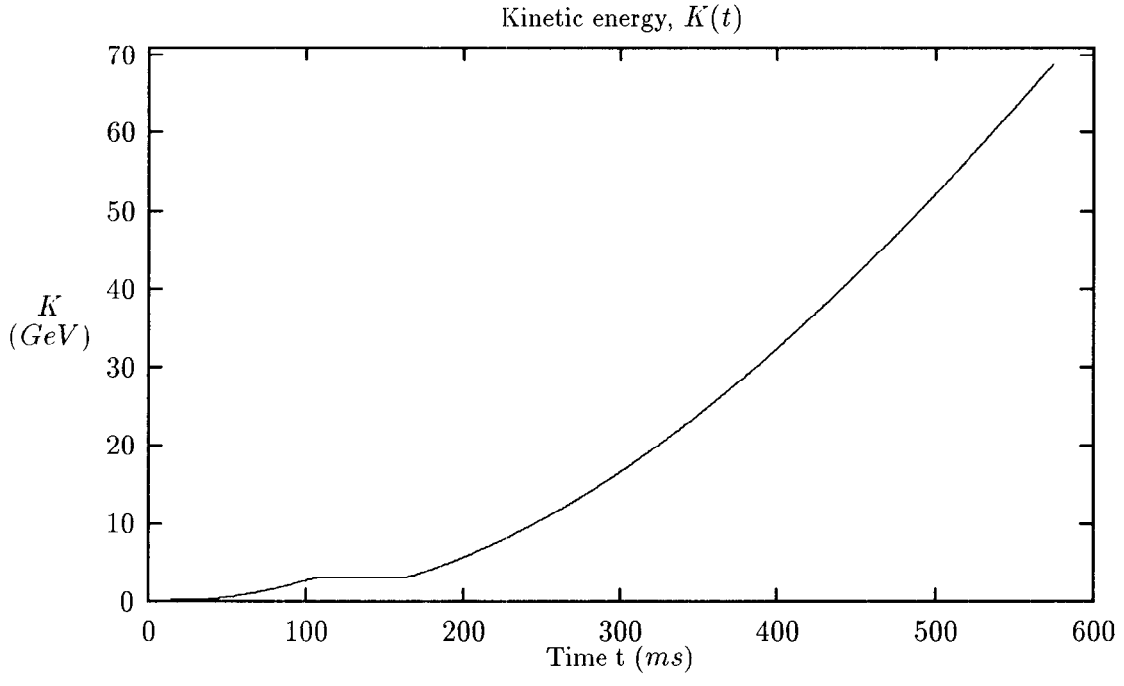

Figure 16: Kinetic energy *vs.* time. $Au^{+33}, h = 9$.

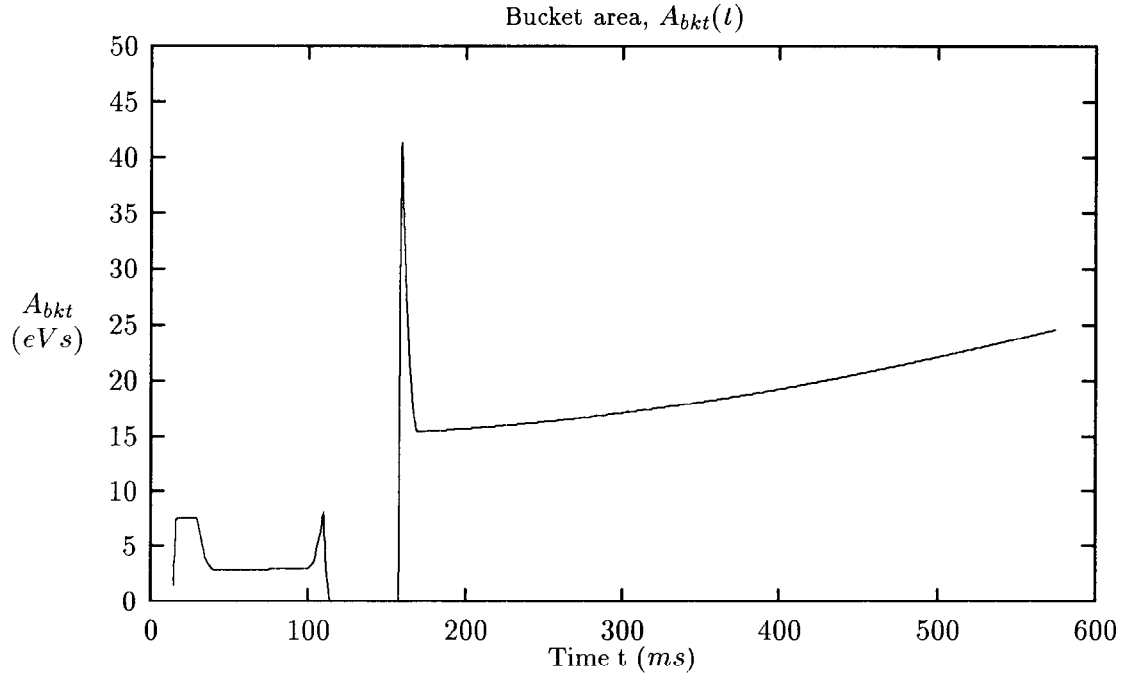

Figure 17: The bucket area *vs.* time. $Au^{+33}, h = 9$.

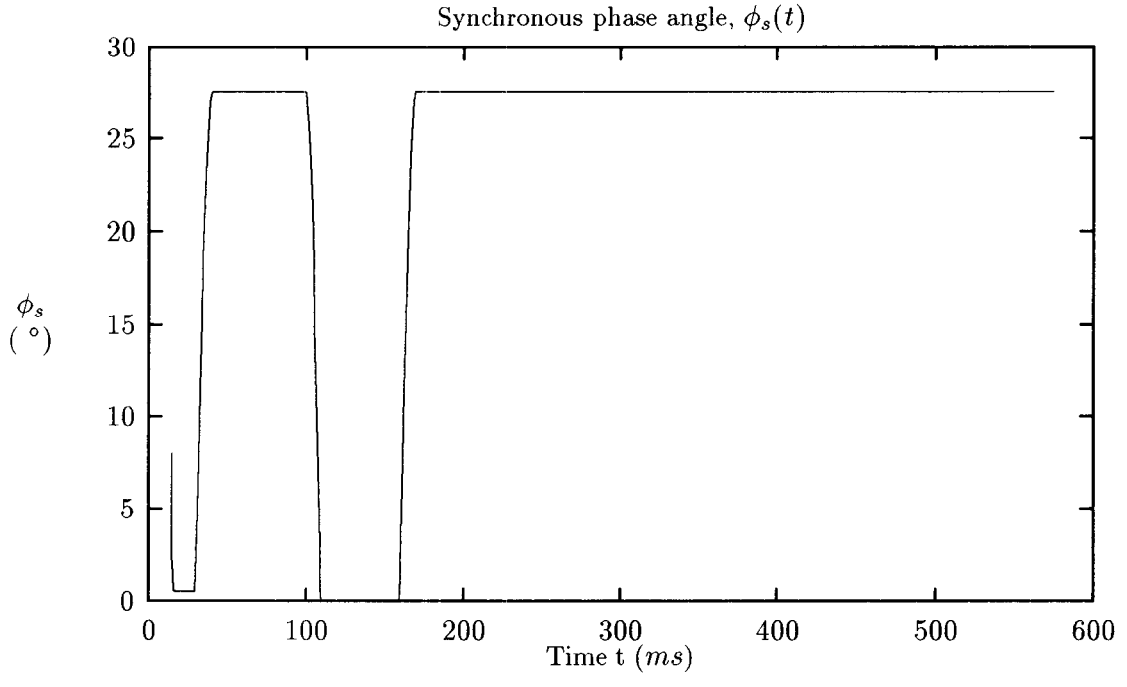

Figure 18: Synchronous phase angle *vs.* time. $Au^{+33}, h = 9$.

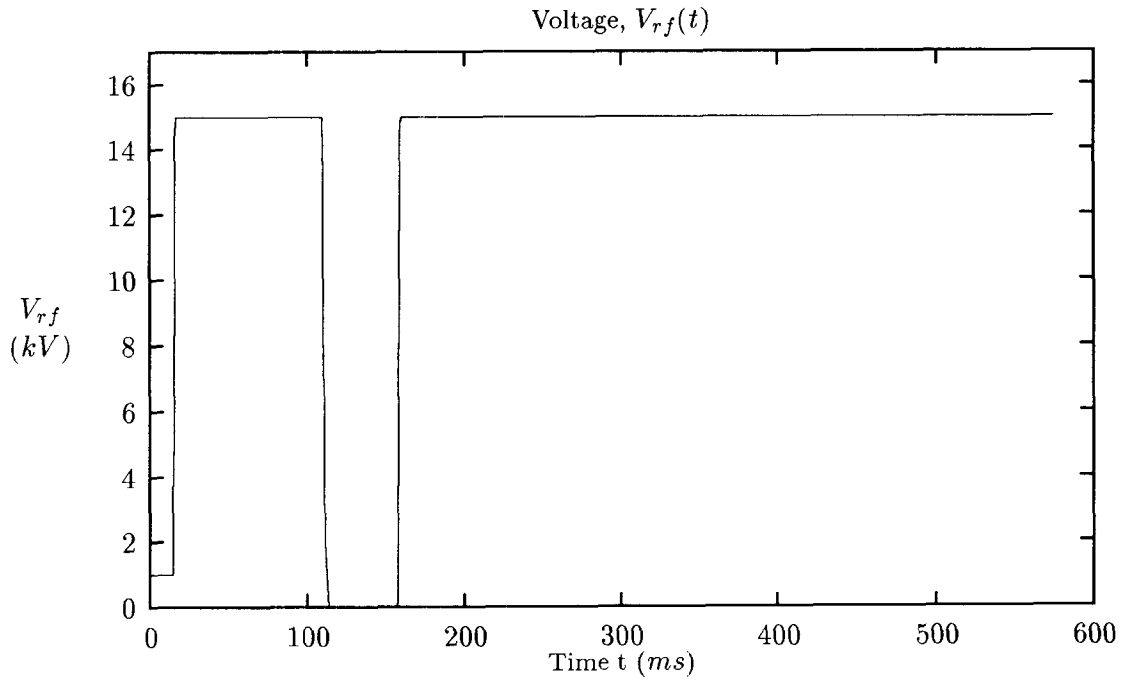

Figure 19: RF voltage *vs.* time. $Au^{+33}, h = 9$.

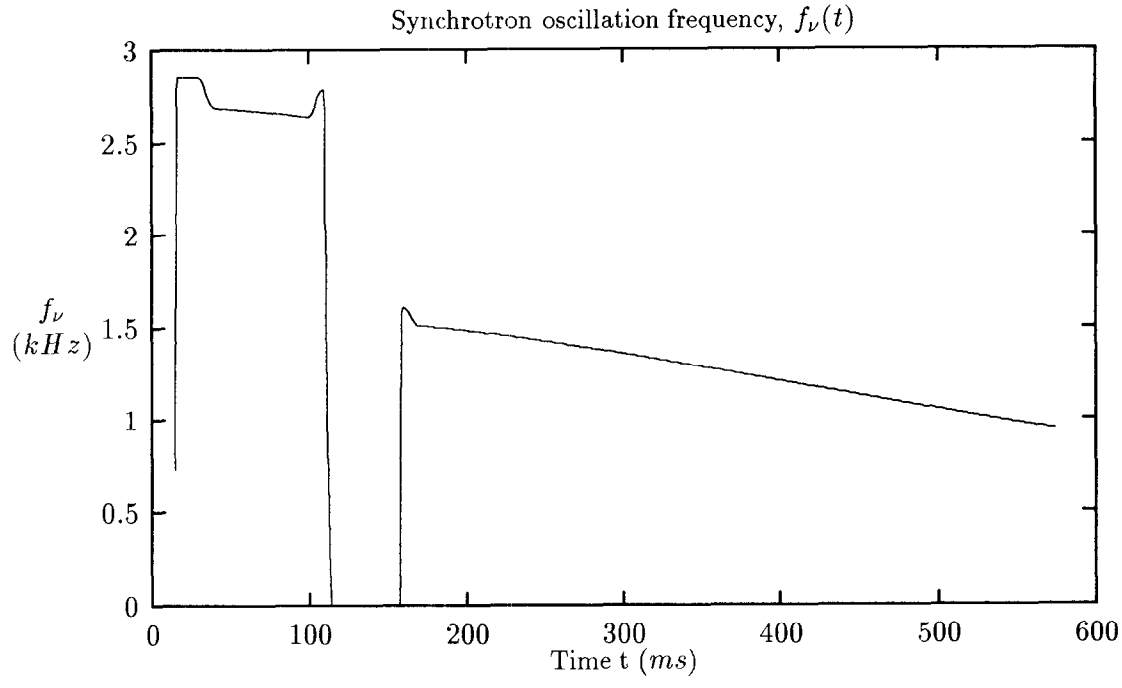

Figure 20: Synchrotron oscillation frequency *vs.* time. $Au^{+33}, h = 9$.

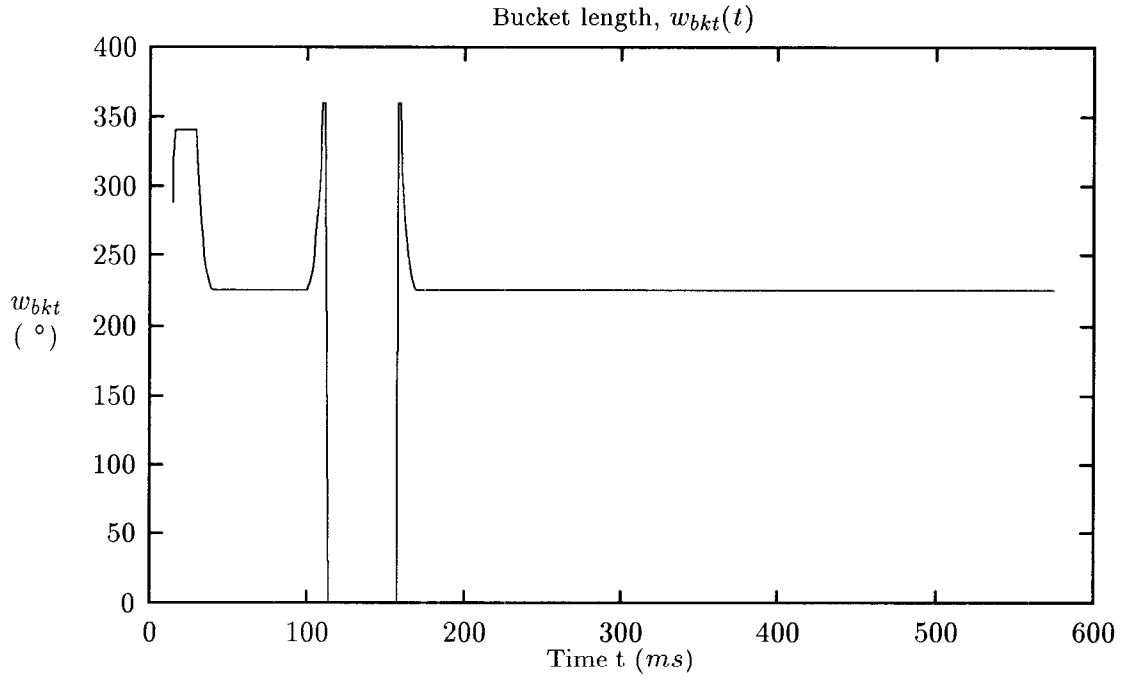

Figure 21: Bucket length (degree) *vs.* time. $Au^{+33}, h = 9$.

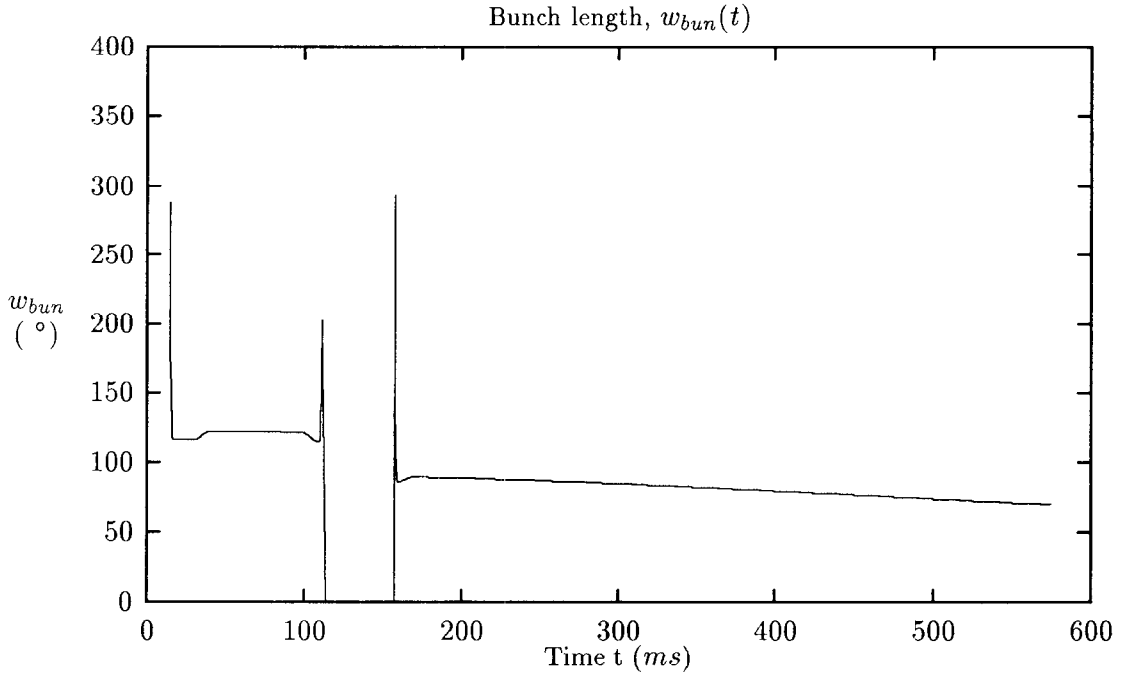

Figure 22: Bunch length (degree) *vs.* time. $Au^{+33}, h = 9$.

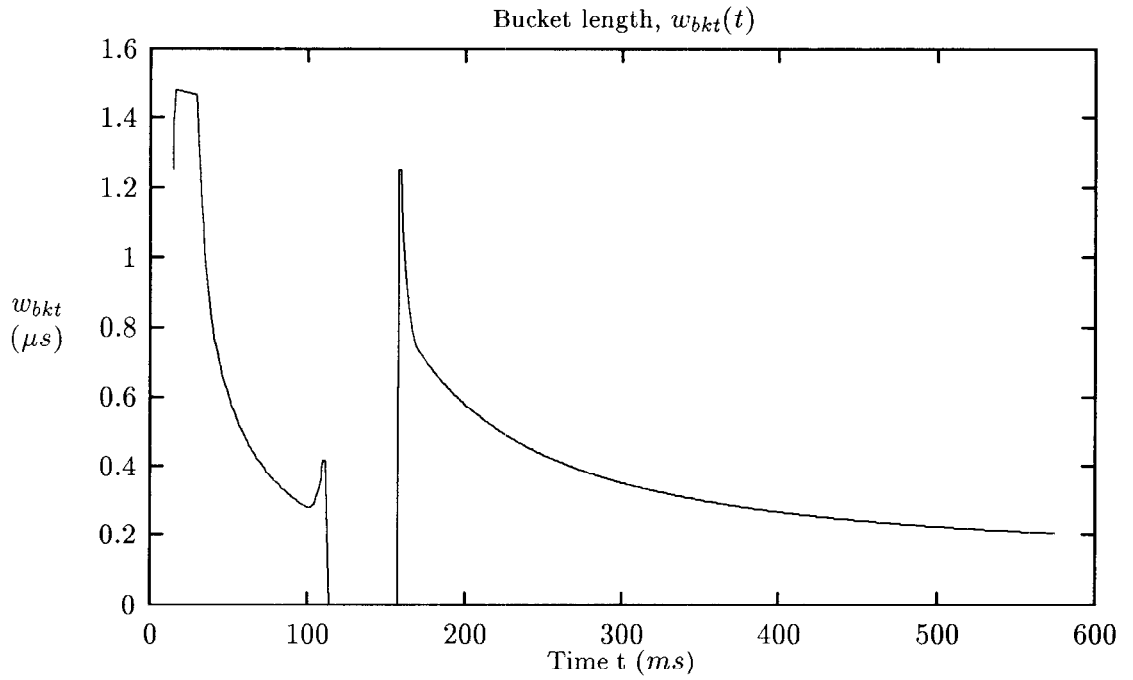

Figure 23: Bucket length (ms) *vs.* time. $Au^{+33}, h = 9$.

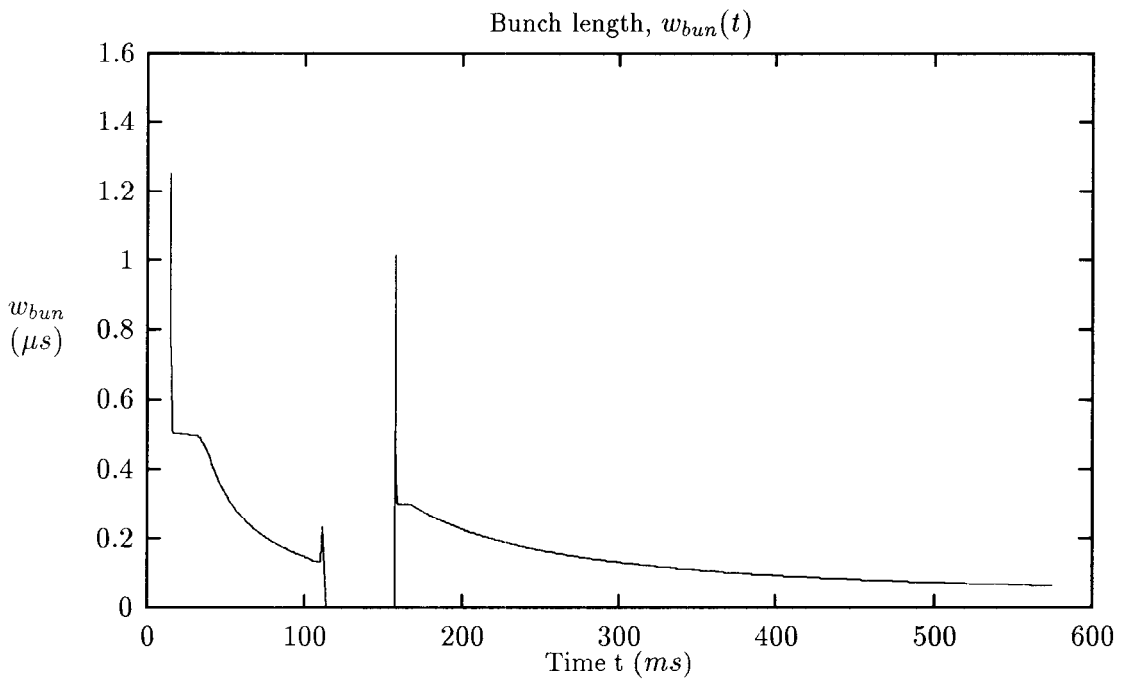

Figure 24: Bunch length (ms) *vs.* time. $Au^{+33}, h = 9$.

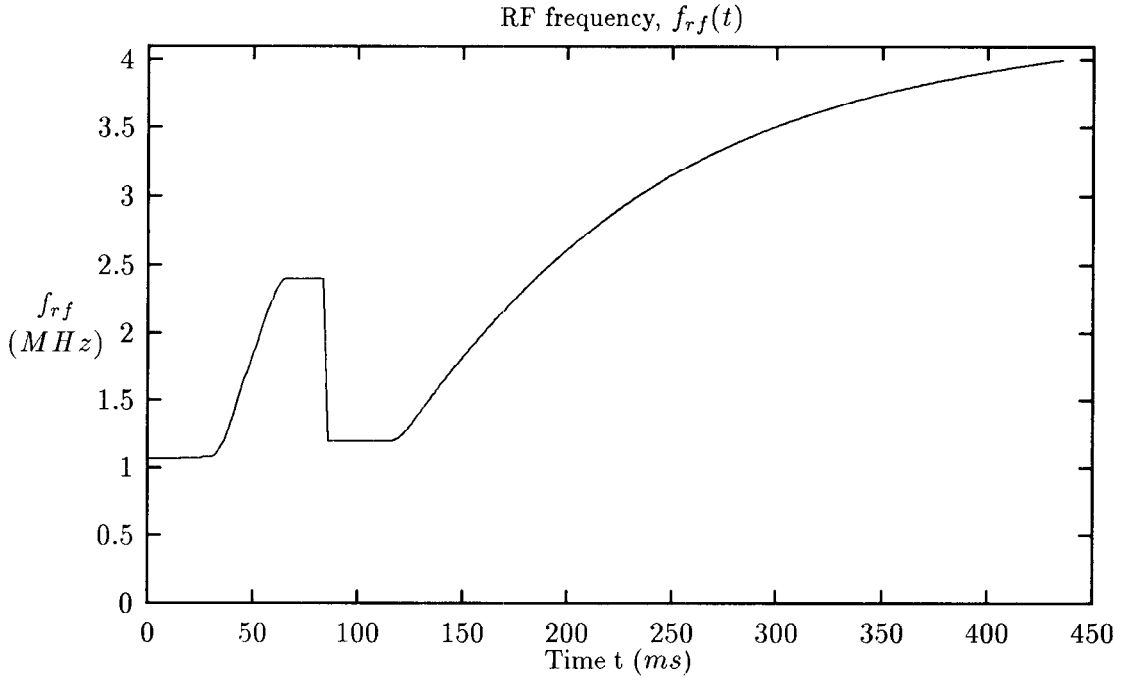

Figure 25: RF frequency *vs.* time. $Si^{+14}, h = 6$.

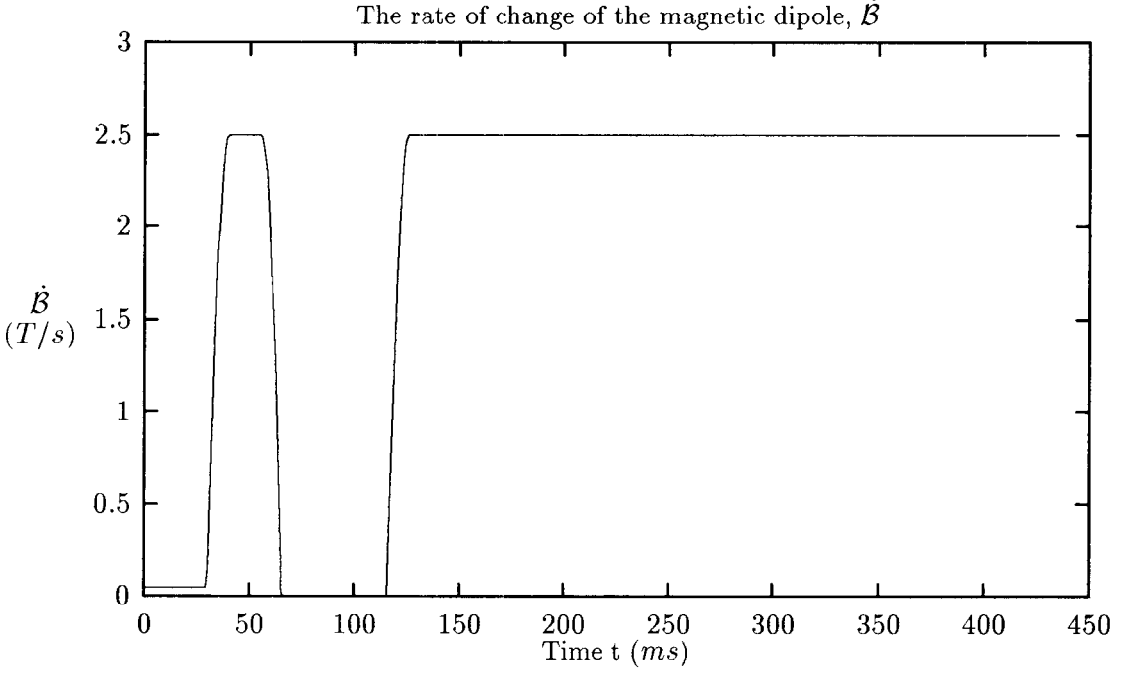

Figure 26: The rate of change of the magnetic dipole field *vs.* time. $Si^{+14}, h = 6$.

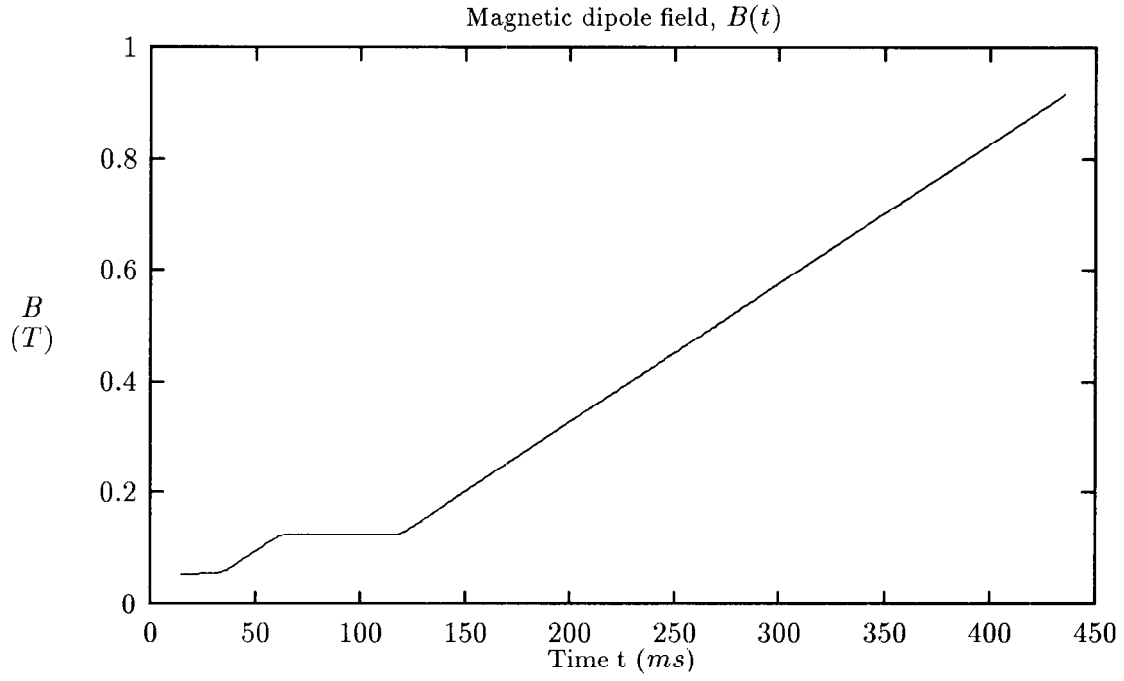

Figure 27: The magnetic dipole field *vs.* time. $Si^{+14}, h = 6$.

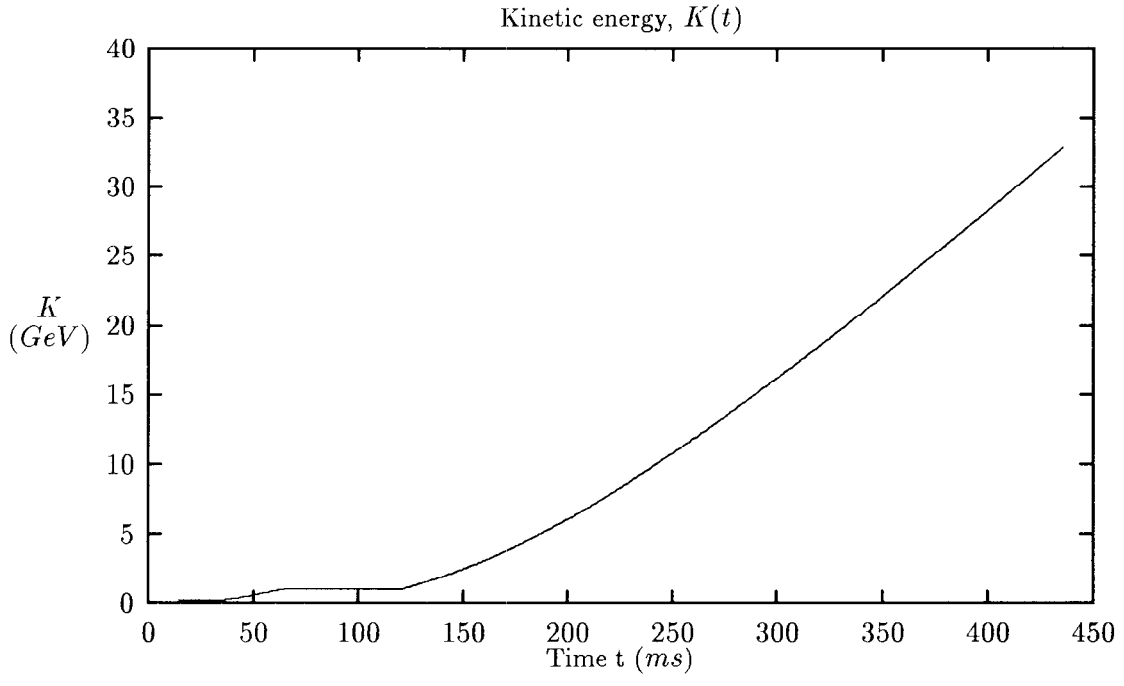

Figure 28: Kinetic energy *vs.* time. $Si^{+14}, h = 6$.

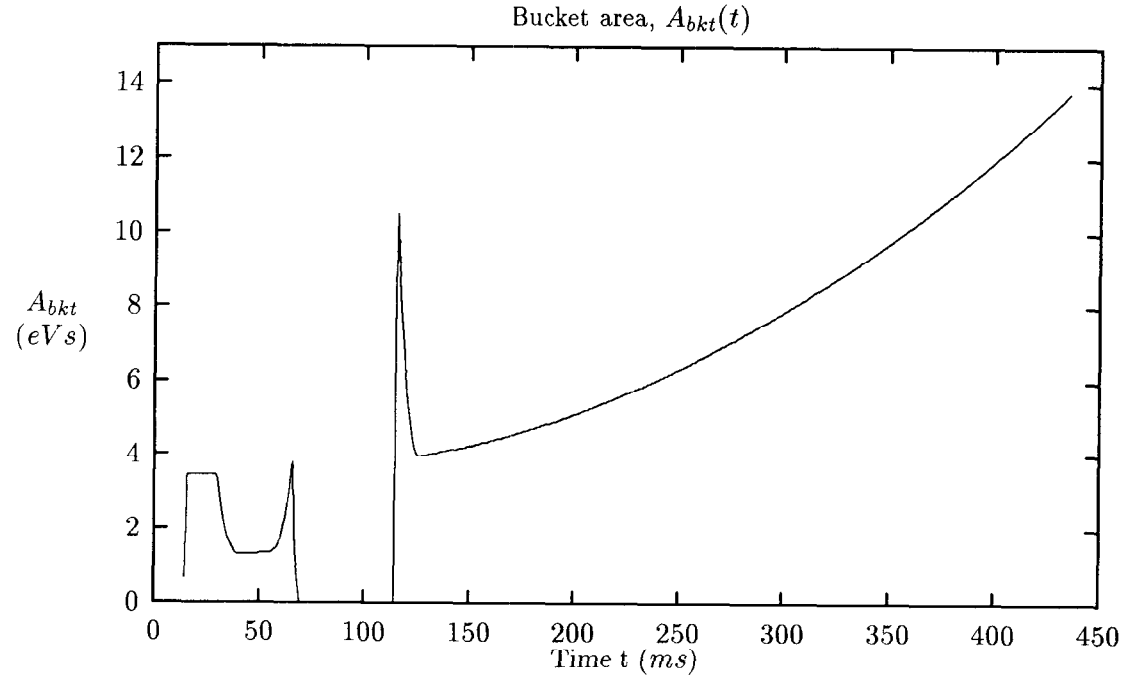

Figure 29: The bucket area *vs.* time. $Si^{+14}, h = 6$.

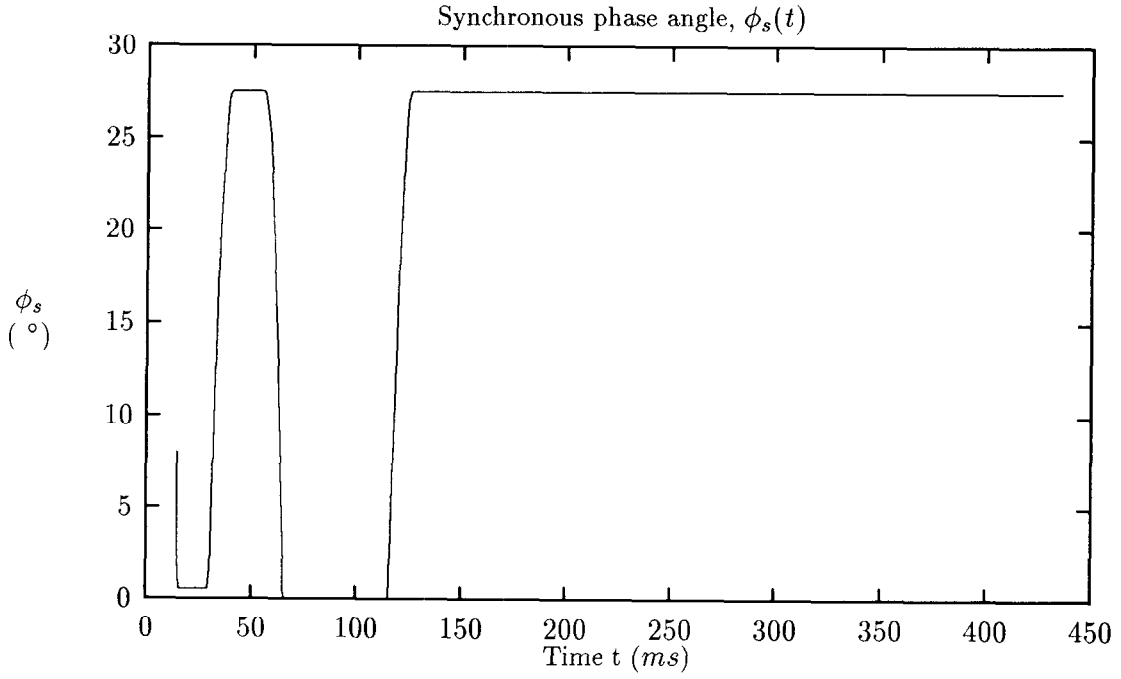

Figure 30: Synchronous phase angle *vs.* time. $Si^{+14}, h = 6$.

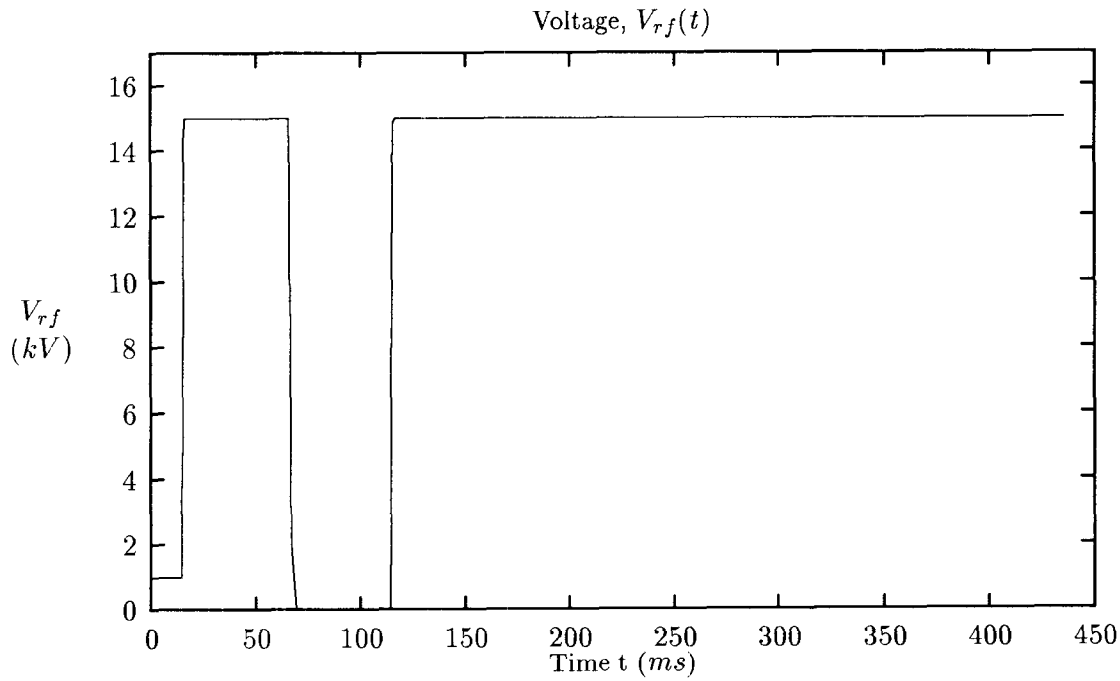

Figure 31: RF voltage *vs.* time. $Si^{+14}, h = 6$.

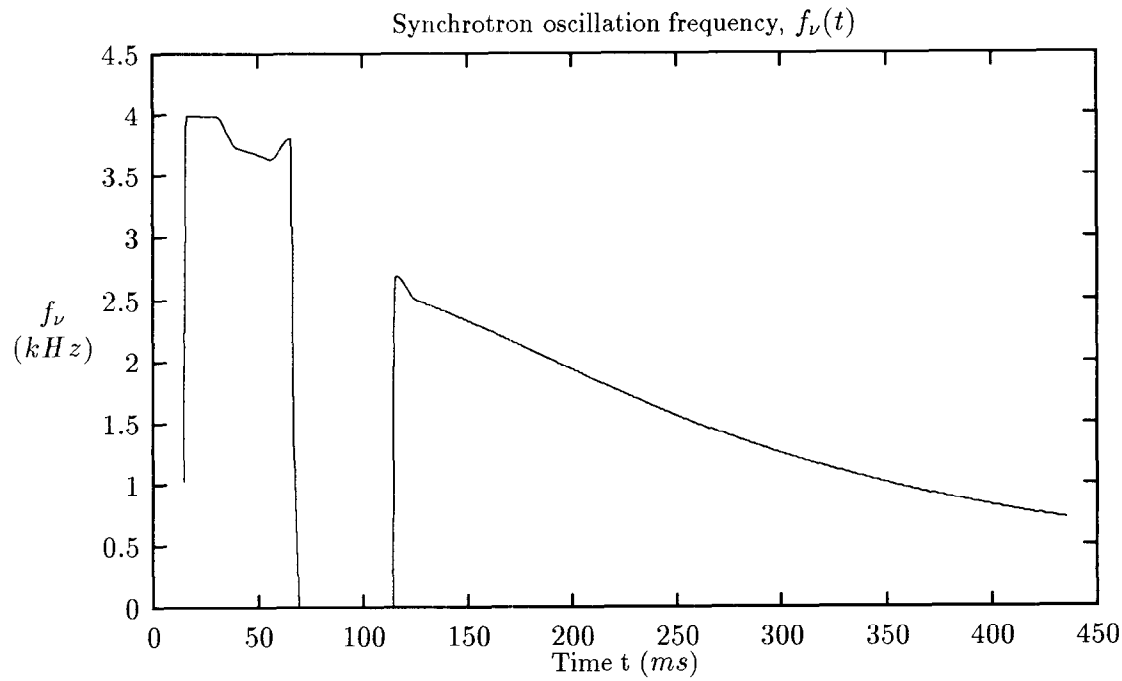

Figure 32: Synchrotron oscillation frequency *vs.* time. $Si^{+14}, h = 6$.

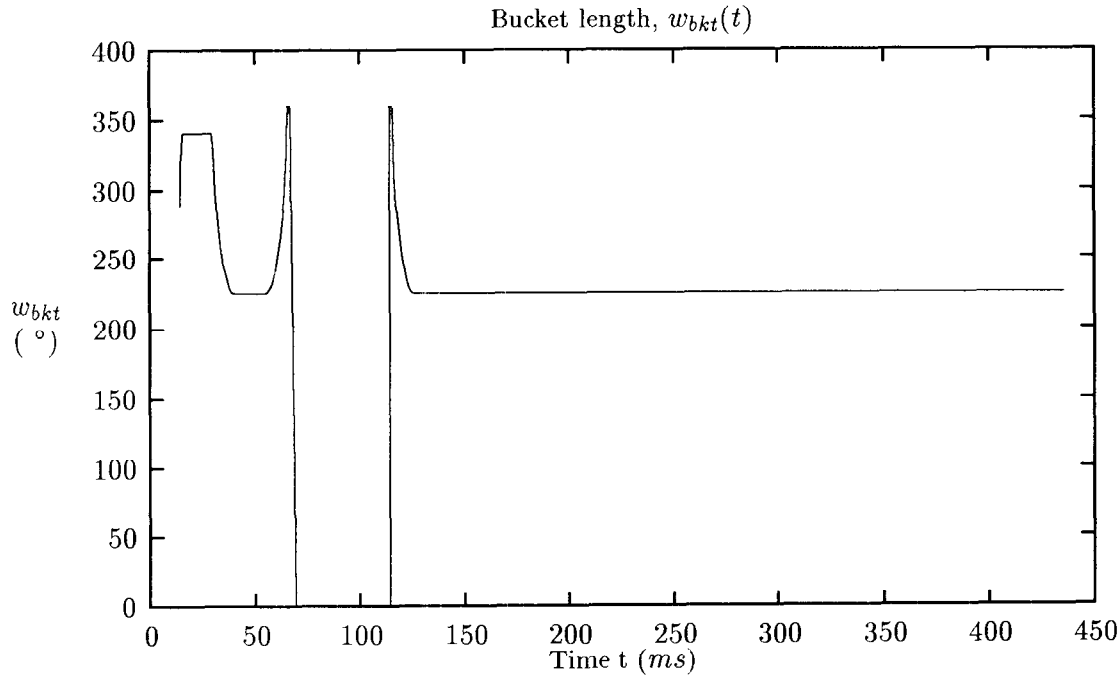

Figure 33: Bucket length (degree) *vs.* time. $Si^{+14}, h = 6$.

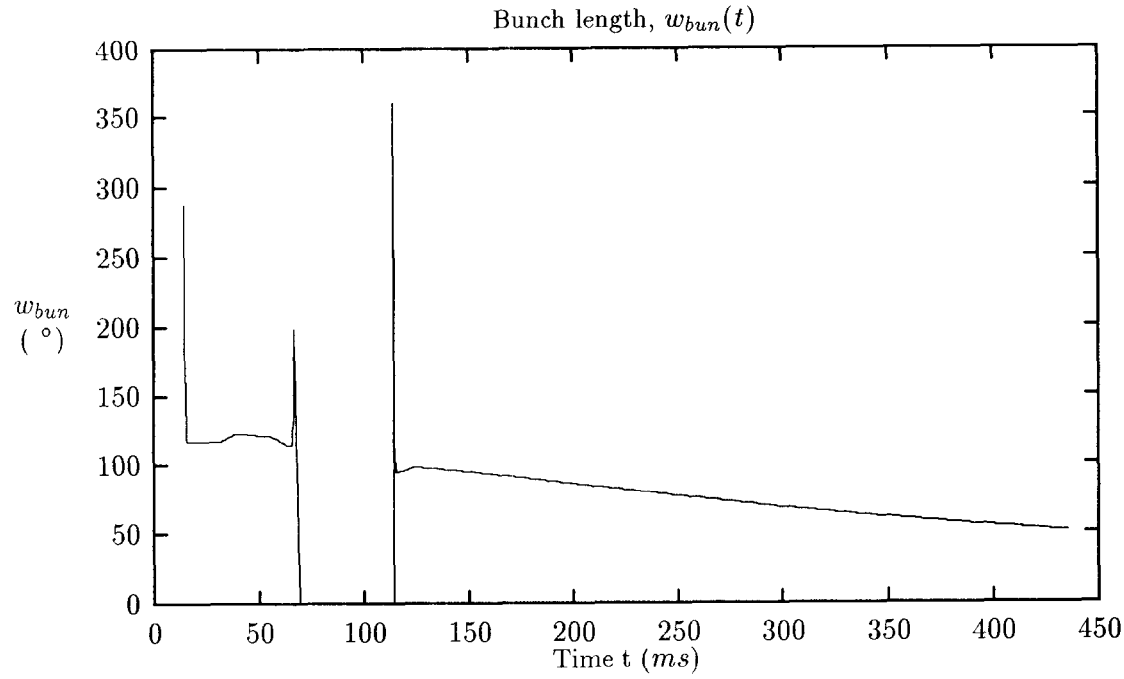

Figure 34: Bunch length (degree) *vs.* time. $Si^{+14}, h = 6$.

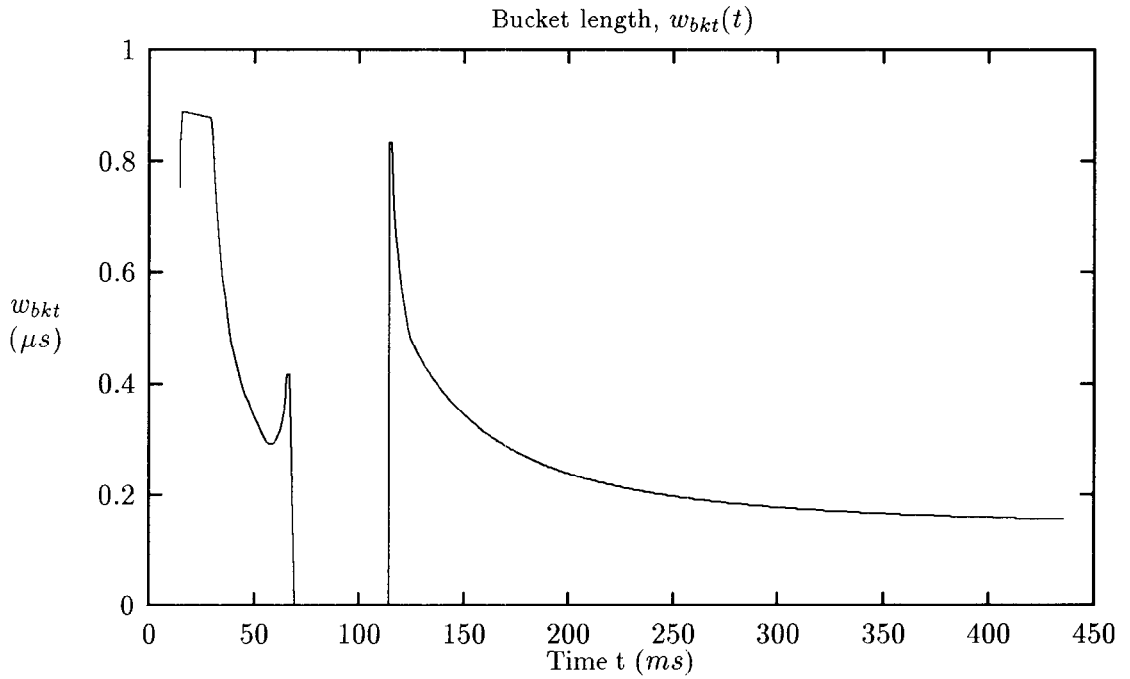

Figure 35: Bucket length (ms) *vs.* time. $Si^{+14}, h = 6$.

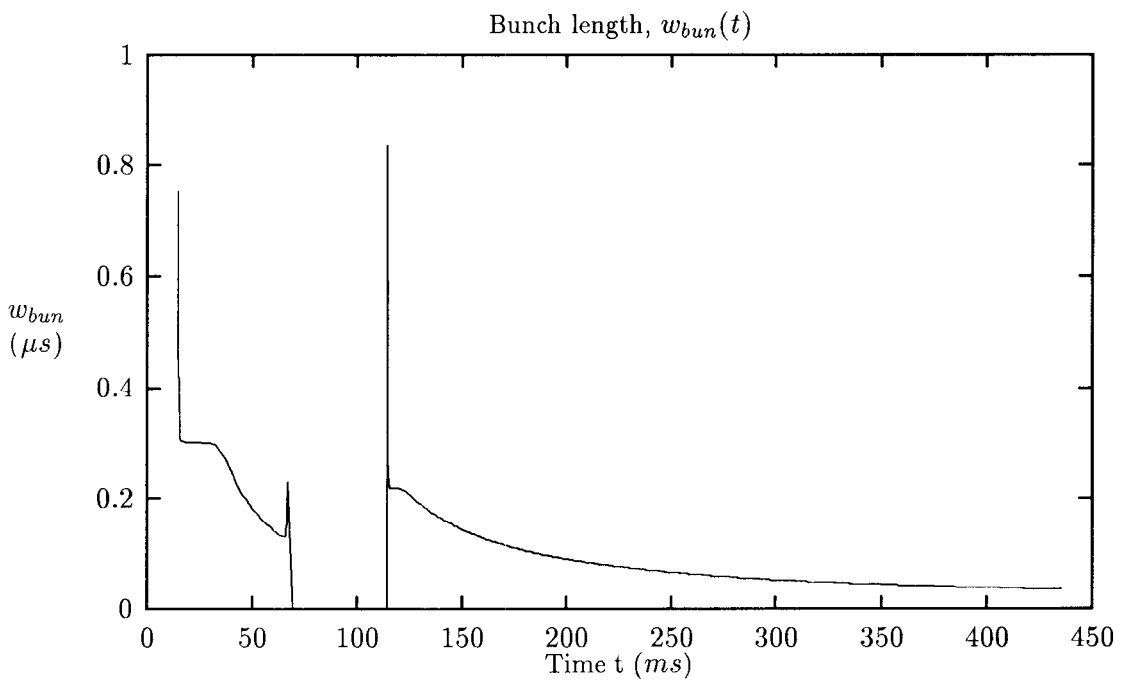

Figure 36: Bunch length (ms) *vs.* time. $Si^{+14}, h = 6$.